Vision Res. Vol. 24, No. 9, pp. 1021–1035, 1984
Printed in Great Britain.

0042-6989/84 $3.00 + 0.00

DETECTION AND IDENTIFICATION OF SPATIAL FREQUENCY: MODELS AND DATA

DEAN YAGER[1], PATRICIA KRAMER[1], MARILYN SHAW[2] and NORMA GRAHAM[3]
[1]Institute for Vision Research, S.U.N.Y. College of Optometry, 100 E. 24th Street, NY 10010, U.S.A.,
[2]Department of Psychology, Rutgers University, New Brunswick, NJ 08903 and Bell Laboratories, Murray Hill, NJ 07974, U.S.A. and [3]Department of Psychology, Columbia University, New York, NY 10027, U.S.A.

(*Received* 15 *April* 1983; *in revised form* 29 *December* 1983)

Abstract—Detection and identification of up to four simple sinusoidal gratings were studied. The experimental results were quantitatively compared to predictions from several models. The models all assumed probabilistically independent channels sensitive to different ranges of spatial frequency. The models differed in the shapes of their underlying distributions and, for detection, their decision rule. Detection and identification of far-apart spatial frequencies were consistent with these models. Thus, uncertainty effects for both detection and identification (the decrease in performance with an increase in the number of possible spatial frequencies) can be explained without assuming that attention capacity is limited.

INTRODUCTION

Spatial-frequency channels models have been quite successful in quantitatively accounting for the detection of visual patterns (e.g. Bergen *et al.*, 1979; Davis *et al.*, 1983; Graham, 1977; Graham *et al.*, 1978; Mostafavi and Sakrison, 1976; Quick *et al.*, 1978; Watson, 1982). Attempts to use these models to explain identification of near-threshold patterns have been encouraging (Hirsch *et al.*, 1982; Nachmias, 1974; Nachmias and Weber, 1975; Olzak, 1981; Thomas and Barker, 1977; Thomas *et al.*, 1982; Watson and Robson, 1981). Many questions remain unanswered, however, about the precise characteristics of the spatial-frequency channels necessary to explain near-threshold pattern vision.

Here we attempt to refine our knowledge of these channels by studying the identification and detection of up to four simple sinusoidal gratings of far-apart spatial frequencies. More specifically, on each trial a sinusoidal grating or a blank was presented. In a given block of trials, the grating's spatial frequency was chosen randomly from a set of one, two, or four frequencies. Neighboring frequencies were either a factor of two or a factor of three apart. After each trial, the observer indicated whether or not he thought he saw a grating at all (the detection response). Also, when the set size was two or four, no matter which detection response had been given, the observer indicated which spatial frequency he thought he saw (the identification response).*.

The detection and identification responses recorded in the experiment were then compared to the quantitative predictions from several models postulating probabilistically independent channels. These comparisons addressed several issues:

(*a*) *Uncertainty effects*: *noisy channels vs limited capacity*

Recently, uncertainty (or set-size) effects in the detection of gratings of up to five different spatial frequencies have been shown to exist (Davis and Graham, 1981; Davis *et al.*, 1983; Graham *et al.*, 1978). That is, a grating is less detectable when the observer is uncertain about its spatial frequency (because trials of several different spatial frequencies are randomly intermixed within a block) than when he is certain (because trials of only one spatial frequency are being presented in that block or because an auditory cue before the trial has indicated the frequency).

According to one kind of explanation of uncertainty effects, the decrements in performance with increased set size are simply the result of the observer's having to monitor more channels, each of which has some independent probability of giving a "false alarm" to an inappropriate stimulus. There is assumed to be no limit to an observer's attention capacity—that is, an observer is perfectly able to monitor many different channels at once, and the responses of the channels are not degraded when more channels are monitored. The factor limiting the observer's performance in larger set sizes is simply the probabilistically independent variability (often called noise) in the responses of different channels which

*Since the possible identification responses did not include "blank", this was not a "complete identification" experiment in the terminology of Bush *et al.* (1963). By ignoring the blank trials, however, this experiment does reduce to a complete identification experiment of the kind that is often called a pure recognition experiment (e.g. Luce, 1963; Green and Birdsall, 1978). The everyday-language connotations of the word "recognition" seem less appropriate than those of "identification", however, and so we have chosen the latter.

leads to increased numbers of false alarms as set size is increased. These models will be called "noise-limited" or "independent-channels" models here. It is this class of models which we quantitatively compare to our empirical results.

A second explanation of uncertainty effects is a fixed attention capacity. Either the observer cannot monitor all the relevant channels at once, at least not perfectly, or else the responses of the channels are degraded when more are monitored. This model will be called "attention-capacity-limited," and will be considered only qualitatively in this paper.

The quantitative results from the previous study of the forced-choice detection of sinusoidal gratings were consistent with noise-limited models (Davis et al., 1983). There was no need to postulate a limited attention capacity; an observer seemed able to monitor up to at least five different spatial-frequency channels perfectly. This consistency provides further support for the existence of independent variability in the responses of spatial-frequency channels, a conclusion previously suggested by summation experiments using compound gratings.

In the present study we measured uncertainty effects for the identification of sinusoidal gratings as well as for detection. We asked whether the sizes of these effects were all consistent with noise-limited models, or was there evidence for limited attention capacity in the potentially more complex task of identification.

This study also provided another opportunity, under slightly different conditions (single-interval trials, set sizes of 1, 2, and 4 with the same observer in the same experiment), to determine whether detection uncertainty effects were consistent with the class of noise-limited models and to narrow the range of possible noise-limited models.

(b) Comparison of detection to identification performance

If there are multiple channels sensitive to different ranges of spatial frequency, and if the responses of different channels remain identifiable upstream in the nervous system and are used as the basis for identification of spatial frequency, there ought to be a close relationship between detection and identification performance. If simple sinusoidal gratings are of different enough frequency to excite separate channels, and if they are of high enough contrast to be easily detectable, they ought also to be easily identifiable. More generally, identification performance ought to depend on detection performance with both improving from chance to perfect over the same range of contrasts.

Previous studies have compared detection and identification from a set of two spatial frequencies in a forced-choice paradigm. [In this "two-by-two" paradigm, one interval of each two-interval trial contained one of the two frequencies; the other interval contained the blank. The observer had to indicate the interval (detection) and the frequency (identification]). In accord with a number of reasonable multiple-channel models, proportion correct identification equals proportion correct detection for spatial frequencies far enough apart to stimulate separate channels (Nachmias and Weber, 1975; Campbell et al., 1976; Thomas and Barker, 1977; Watson and Robson, 1981).

Here we again ask whether detection and identification performances are related to each other in a manner consistent with multiple-channels models, but this study includes a set size of four as well as of two and uses single-interval trials rather than the two-by-two paradigm. We also compare detection performance in a set size of one to identification performances in set sizes of two and four.

(c) Are there systematic confusions among the identification responses to far-apart spatial frequencies?

If spatial frequencies a factor of two or three apart (like those used in this study) stimulate completely separate channels, and if the responses of those channels remain separate upstream, an observer ought to show no systematic confusions among the identification responses to different frequencies. That is, when he is wrong about a grating, he ought to be no more likely to call it a near spatial frequency than a far-away spatial frequency. Using a set size of four allowed us to check for the presence or absence of systematic confusions in the identification responses.

INDEPENDENT-CHANNELS MODELS OF DETECTION AND IDENTIFICATION

The predictions from several versions of models postulating probabilistically-independent channels were compared to the results from this study; these models are presented as a representative sample of independent-channel models that are reasonable in light of current evidence. Predictions of other possible versions are briefly described in the Discussion.

Assumptions of models

(1) Multiple channels. Spatial information in the human visual system is analyzed by multiple channels, each of which is sensitive to patterns that contain spatial frequencies in a restricted range. The output of an individual channel on an individual trial can be represented as a single number.

(2) Completely separate channels. Although the spatial-frequency ranges for different channels overlap and there may or may not be direct excitation and inhibition among some channels, if frequencies are sufficiently far apart, no channel will respond to more than one of the frequencies.

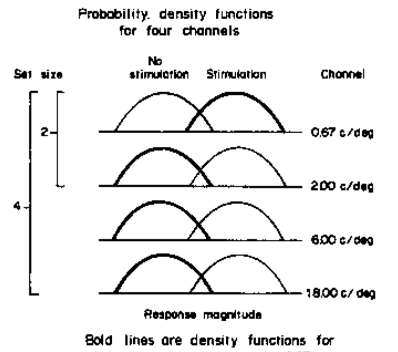

Fig. 1. Schematic probability density functions for the responses of 4 channels to no stimulus and to a stimulus. The distributions are identical for all channels since the stimuli are assumed to be equally detectable. In the example shown, the responses of the 2.0, 6.0, and 18.0 c/deg channels to the 0.67 stimulus are the same as the noise distributions (assumption 2 in the text).

(*3*) *Independent variability.* There is variability over trials in the output of any channel to any pattern. This assumption is illustrated in Fig. 1 by the schematic probability density functions describing the distribution of responses by each of four channels to blank (noise) and grating (signal) stimuli. (See figure legend for further description.) Further, the outputs of different channels (sources of noise) are probabilistically independent. That is, the probability that two channel outputs are greater than criterion on a single trial is the product of the probabilities that each channel output is greater than criterion.

Assumptions (2) and (3) together are equivalent to what is sometimes called "orthogonal channels."

In the models quantitatively compared to our experimental results, the probability density functions describing the variability in the response of any single channel to any pattern could either be exponential or Gaussian.

(*3a*) In the exponential case, the probability density functions are zero for values of response magnitude x less than zero and are equal to $\exp(-kx)$ for values of response magnitude x above zero. The value of k determines the channel's sensitivity with lower k's corresponding to higher sensitivity. For the blank stimulus, k equals 1.0.

We have defined a parameter $\underline{k}'$, equal to $2 \log_{10} (1/k)$, that is more convenient to use than k. Not only do higher values correspond to greater sensitivity (with a value of zero for the blank) but in certain situations (see appendix) its values are quite close to values of $\underline{d}'$, the parameter used to characterize models assuming Gaussian distributions.

The exponential distribution may seem a bit peculiar as a description of the response of sensory channels, but the ROC curves it predicts are like those measured so far (e.g. Green and Swets, 1974; appendix here), being nearly linear on z-axes and getting shallower with increased detectability. Further, exponential density functions are tractable in a way Gaussians are not since they can be integrated analytically (see appendix).

(*3b*) In the case of Gaussian distributions, only the case where the variances in response to noise (blanks) and signals (gratings) are equal is quantitatively compared to our results. Cases where the variance in response to signals is somewhat greater than that in response to noise are discussed later, however. The parameter used to characterize the model with Gaussian distributions is d'. It equals the difference between the means of the distribution divided by the standard deviation of either.

(*4*) *Perfect monitoring.* The observer is assumed to base his responses on (that is, to monitor) only those channels that are relevant in a particular condition. Thus when the set size is one ($M = 1$ in an alone block of trials), the observer monitors only the channel sensitive to the one frequency being presented in that block. Similarly when the set size is two or four ($M = 2$ or 4 in an intermixed block of trials) the observer monitors only 2 or 4 channels, respectively. It is further assumed that the channels' responses are unchanged by being monitored.*

(*5*) *Detection linking hypotheses.* Two versions of an assumption linking the observer's detection response ("yes" or "no") to the output of the channels were considered here. When the set size M equals one (the alone condition) the two are indistinguishable in their predictions.

(*5a*) *Maximum-output detection rule.* The observer says yes if and only if the maximum of the outputs from all monitored channels is greater than some criterion (alternately, if and only if the response of at least one monitored channel is greater than a criterion, where the criterion is constant across channels). At least when the distributions are Gaussians of equal variance, this maximum-output linking hypothesis leads to predictions for these experiments that are very close to those assuming an ideal observer (Nolte and Jaarsma, 1967).

(*5a*) *Adding-of-outputs detection rule.* The observer says yes if and only if the sum of the outputs from all monitored channels is greater than a criterion.

These two versions can be seen as extreme members of a whole family of combination rules differing in the extent to which the greater-valued outputs are emphasized relative to the lesser-valued outputs. The adding-of-outputs rule weights all sizes of output

*Whether the observer monitors exactly one channel per stimulus or several channels per stimulus (e.g. several channels with overlapping sensitivities all sensitive to one spatial frequency) is irrelevant, everything else remaining constant. To avoid constant terminological difficulties in the text, however, the observer will be assumed to monitor exactly one channel per stimulus.

equally; the maximum output rule totally ignores all but the largest.*

(*6*) *Identification linking hypothesis.* Only one version of an identification linking assumption was considered here, a maximum-output identification rule. In particular, an observer identifies a stimulus as being of the frequency corresponding to the channel which gives the largest response on that trial.

Predictions of models

Quantitative predictions can be calculated from these models when the spatial frequencies are far-enough apart to stimulate completely separate channels (see Appendix). In the Results section, our experimental results are explicitly compared with three (but, in effect, all four) of the models described in the above assumptions. For convenience, they are given short names:

(1) The Adding-of-Gaussians model assumes equal-variance Gaussians with an adding-of-outputs detection rule.

(2) The Maximum-Gaussian model assumes equal-variance gaussians and a maximum-output detection rule.

(3) The Maximum-Exponential model assumes exponentials and a maximum-output detection rule.

The predictions of a fourth model—an Adding-of-Exponentials model—are very similar to those of the Maximum-Exponential model (Graham *et al.*, 1983).

EXPERIMENTAL METHODS

Stimuli

The stimuli were vertically oriented sinusoidal gratings produced on the face of an oscilloscope (Tektronix 5103N) by a conventional z-axis modulation technique (Campbell and Green, 1965). This instrument had a P-31 phosphor of a desaturated green hue. The rectangular display subtended 5.25 deg horizontal and 4.0 deg vertical and was viewed binocularly from a distance of 57 in. A 12.5 deg diameter circular surround of approximately the same hue and brightness framed the display. The display had a mean luminance of 6.1 cd/m^2.

On each trial, either a stimulus or a blank was presented for 185 msec. The stimuli had abrupt onsets and offsets. Between presentations of stimuli the screen was uniformly illuminated at the mean luminance.

Stimulus presentation was under control of the observer, and an auditory signal was coincident with the stimulus or blank on each trial.

Procedure

Three experimental conditions were used, determined by the number, M, of alternative spatial frequencies that might be presented. In the alone condition ($M = 1$, where either a blank or a given spatial frequency was presented on each trial), observers reported whether anything was seen (detection response). In the intermixed conditions ($M = 2$, where either a blank or one of two spatial frequencies was presented on each trial, and $M = 4$, where either a blank or one of four spatial frequencies was presented on each trial), the observer reported whether anything was seen (detection response), and the observer also reported which frequency was presented (identification response) independently of the detection response; that is, even if the detection response was "no."

Spatial frequencies

The spatial frequencies were drawn from two groups. In the group called 3X, adjacent frequencies differed by a factor of three; they were 0.67, 2.0, 6.0, and 18.0 c/deg. In the group called 2X, adjacent frequencies differed by a factor of two; they were 1.0, 2.0, 4.0, and 8.0 c/deg.

Contrasts

Based on results from preliminary sessions, the contrasts were set so that all frequencies would yield approximately equal detectability in the alone condition. Throughout a triad of sessions (see below), the contrasts were kept constant. The level of detectability in different triads of sessions was deliberately varied.

Details of the sequence of trials and sessions

Sessions were generally run in triads, as follows. One session was the alone condition ($M = 1$), in which four blocks of 300 trials were run. In each block, a given grating was presented on 200 trials, randomly intermixed (without replacement) with 100 blank trials. A different spatial frequency was used in each of the four blocks. In the other two sessions, there were intermixed conditions. Again four blocks of 300 trials were run each session. Two of the blocks in each session were two-frequency ($M = 2$) intermixed blocks, in which two frequencies of a group of four were presented in the first block, and the other two frequencies in the second block; in a block each grating was presented 100 times, and there were 100 blank trials. The other two blocks in each session were four-frequency intermixed ($M = 4$); in each of these two blocks each of the four frequencies in the

*Shaw (1982) also computes predictions using these decision rules. However, the terminology differs from that used here. The maximum output decision rule is equivalent to second-order integration with either continuous or discrete distributions and fixed sharing. The observer says yes if one or more channels exceed a criterion. The adding-of-outputs decision rule is equivalent to first-order integration with continuous distributions and fixed sharing. The observer says yes if the sum of the equally-weighted outputs from the channels exceeds a criterion.

group was presented on 50 trials, and there were 100 blank trials. In general, different sessions were run on different days. In a triad, the alone session sometimes preceded and sometimes followed the intermixed sessions.

The order of blocks within sessions was counterbalanced; a 5-min period of dark adaptation preceded each block; and there were 30 practice trials at the beginning of each block which were not included in the analyses. No feedback was given since this could have led the observer to attend to irrelevant cues, such as small contrast differences.

For both D.Y. and P.W. the sessions using the 2X group of frequencies were run after the sessions for the 3X group of frequencies had been completed. Observer E.G., who was run first, participated only in intermixed sessions, and only identification results were collected from him.

The following pairings of frequencies were used in the two-frequency ($M = 2$) intermixed blocks: with the 2X group of spatial frequencies (for all observers) 1.0 was always paired with 2.0 and 4.0 was always paired with 8.0 c/deg. With the 3X group of spatial frequencies, for observer P.W., 0.67 was always paired with 2.0, and 6.0 was always paired with 18.0 c/deg. For observer D.Y., that same pairing was used in two intermixed sessions, but in the other six intermixed sessions, 0.67 was paired with 6.0, and 2.0 was paired with 18.0 c/deg. The numbers of sessions run for each observer are indicated in Table 2.

Observers

Three observers' results are reported here: one observer (D.Y.) is an author of this paper and the other two were not aware of the purpose of these experiments. All three had normal visual acuity, with the appropriate correction. (A fourth observer's results are not reported due to several anomalies: not only did she have an uncorrected visual deficit which was unknown to us at the time she was running in the experiment, she also exhibited high inter-session variability and no apparent uncertainty effects, not even for identification.)

RESULTS

Confusion in the identification of spatial frequency

As a check on whether or not our stimuli were detected by completely separate spatial-frequency channels, we looked for systematic confusions among the stimuli. That is, when an observer incorrectly names a frequency, is he more likely to call it a nearby spatial frequency than a far away spatial frequency? We made a tabulation of the four possible identification responses to each of the five stimuli (four gratings plus the blank) in the four-frequency ($M = 4$) intermixed condition. The identification responses to the blank will be discussed in the next section.

Figure 2 shows the tabulations for all three observers (different rows) with both the 3X (left column) and 2X (right column) groups of frequencies; each point is the proportion of trials on which a particular response was given. Three panels of this figure show complete absence of any systematic confusions: the lower two (D.Y.-2X and D.Y.-3X), and the middle left (P.W.-3X). In the other two panels, however, there is some evidence of systematic confusion, rather slight for P.W.-2X and quite pronounced for E.G.-2X.

These results are consistent with the independent-channels models (assumptions 1 to 6 above) if the following assumptions about channel bandwidths are made: channel bandwidths for E.G. are wide enough that an individual channel responds significantly to frequencies a factor of two apart, those for P.W. are somewhat narrower but still encompass frequencies a factor of two apart, and those for D.Y. are narrow enough that frequencies a factor of two apart fall in different channels.

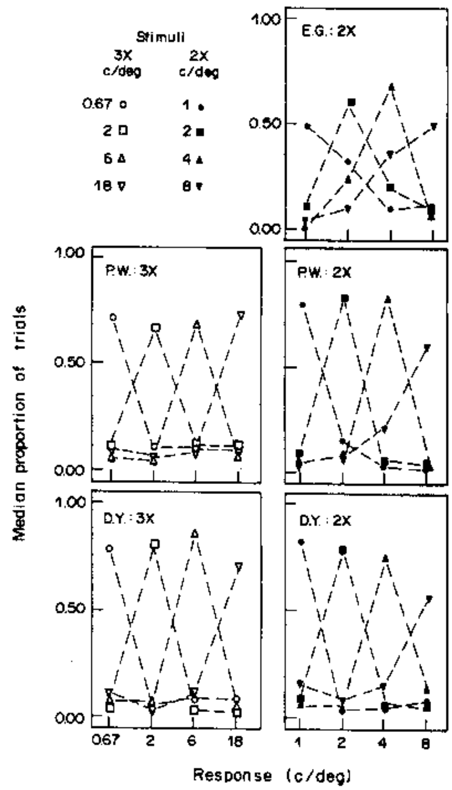

Fig. 2. Median proportions of identification responses to each stimulus. Four frequency ($M = 4$) condition, for the $3\times$ (left) and $2\times$ (right) groups of frequencies. The stimulus is indicated by the symbol (see inset). The identification response is plotted on the horizontal axis. The vertical axis plots the median proportion of all trails of a particular stimulus on which a particular identification response was given.

Alternately, of course, all bandwidths may be so narrow that frequencies a factor of two apart fall into different channels, but for some observers confusions may occur at higher levels of the nervous system (violating the maximum-output identification rule).

In previous psychophysical studies of many sorts, including simultaneous detection and identification of spatial frequencies in a two-by-two forced-choice paradigm (Campbell *et al.*, 1976; Thomas and Barker, 1977; Watson and Robson, 1981) and identification of components in near-threshold compound gratings (Nachmias, 1974; Hirsch *et al.*, 1982; Olzak, 1981) spatial frequencies a factor of three or more apart (in temporal conditions like those here) have appeared to stimulate separate channels, although there is sometimes evidence of negative interaction (perhaps inhibition) between them. Frequencies a factor of two apart, however, sometimes produce marginal results as they did here.

Identification responses to the blank stimulus

The detection and identification rules (assumptions 5 and 6) in the models described above imply that the observer treats all monitored channels equally on any one observation, not biasing his responses toward one frequency or another. Although this implication cannot be tested directly for detection performance, it can be tested for identification. For, if true, the identification responses given to the blank stimulus should be equally distributed among the M alternative responses, except for statistical variation.

Each row of Table 1 shows the average proportions of identification responses to the blank for one observer with the two groups of frequencies. Note that the proportions for $M = 2$ and $M = 4$ were near 0.50 and 0.25, respectively, since there were two and four response alternatives in those conditions, respectively.

As can be seen in Table 1, the four different identification responses to the blank were nearly equally distributed. There are no cases, for example, where one response was almost never given. P.W.'s responses were particularly uniform. For the other two observers, there are some cases where one response was given more often than another. In individual sessions for all three observers there were sometimes rather large nonuniformities of one kind or another which may be more than chance variation. Ideally, therefore, one would modify the above detection and identification rules (assumptions 5 and 6) to allow for differential criteria in the different channels. The fits of the models to the results discussed in the next sections could only be improved. To do so, however, would be a very great deal of work, and it is unlikely that the fits would be much improved thereby. As will be discussed below, we did one further check that a particular discrepancy in the fits of all the models was not due to differential criteria in different channels.

Overview—detection and identification performances

We collected five different kinds of performance data: identification performance (proportion correct) when either two frequencies ($M = 2$) or four frequencies ($M = 4$) were intermixed, and detection performance (hit and false-alarm rates) when one frequency ($M = 1$) was alone in a block, and when either two ($M = 2$) or four ($M = 4$) frequencies were intermixed. The next few sections examine the observed relations among these five kinds of data and compare them to the relations predicted from the independent-channels models described above (assumptions 1–6).

In brief, the models' predictions agree quite well with the experimental results for the observers and sets of frequencies where there were no systematic confusions in Fig. 2. Failure in cases where there is systematic confusion is to be expected, of course, since systematic confusion implies a violation of at least assumption 2 (completely separate channels) or assumption 6 (the maximum-output identification rule). All specific versions of the models fail at some comparisons, however, and all versions mispredict slightly the relation between detection in the alone condition ($M = 1$) and identification in the intermixed conditions ($M = 2$ and 4).

Since the comparisons with theoretical predictions that are described in the succeeding sections tend to disguise the experimental results themselves, the experimental results are given in numerical form in Table 2. Each row in the table is from a different triad of sessions. The left part of the table is from the alone session, the middle part from the first intermixed session, and the right part from the second intermixed session of that triad. In the intermixed sessions,

Table 1. Identification responses to the blank stimulus

	$M = 2$				$M = 4$			
	0.67	2.0	6.0	18.0	0.67	2.0	6.0	18.0
P.W.	0.48(0.02)	0.52(0.02)	0.52(0.01)	0.48(0.01)	0.22(0.01)	0.24(0.01)	0.30(0.01)	0.23(0.02)
D.Y.	0.58(0.04)	0.47(0.03)	0.46(0.04)	0.49(0.02)	0.29(0.02)	0.21(0.01)	0.29(0.03)	0.22(0.02)
	1.0	2.0	4.0	8.0	1.0	2.0	4.0	8.0
EG	0.54(0.03)	0.46(0.03)	0.50(0.04)	0.50(0.04)	0.13(0.02)	0.27(0.02)	0.30(0.01)	0.30(0.02)
P.W.	0.50(0.01)	0.50(0.01)	0.55(0.03)	0.45(0.03)	0.24(0.01)	0.26(0.01)	0.28(0.01)	0.22(0.01)
D.Y.	0.60(0.03)	0.40(0.03)	0.52(0.03)	0.48(0.03)	0.35(0.04)	0.17(0.02)	0.25(0.02)	0.23(0.02)

Identification responses to the blank stimulus. Each row shows the average proportions (and standard errors) of identification responses to the blank for each observer with the 3X (top) or 2X (bottom) group of frequencies. Left panel, $M = 2$. Right panel, $M = 4$. Data are averaged across 4 to 8 sessions.

Table 2. Performance data

	Alone		Intermixed I						Intermixed II					
			2-frequency			4-frequency			2-frequency			4-frequency		
Triad	H	FA	H	FA	%C	H	FA	%C	H	FA	%C	H	FA	%C
D.Y.-3 ×	0.97	0.05	0.92	0.17	97	0.92	0.13	95	0.86	0.17	94	0.93	0.09	97
D.Y.–3 ×	0.94	0.08	0.83	0.09	95	0.83	0.13	91	0.82	0.16	93	0.74	0.16	84
D.Y.–3 ×	0.72	0.21	0.56	0.16	82	0.56	0.28	64	0.62	0.20	81	0.49	0.26	67
D.Y.–3 ×	0.79	0.14	0.57	0.26	80	0.43	0.13	61	0.55	0.12	84	0.50	0.14	71
P.W.–3 ×	0.41	0.02	0.69	0.01	83	0.66	0.07	74	0.64	0.02	81	0.54	0.03	65
P.W.–3 ×	0.77	0.08	0.75	0.05	87	0.76	0.07	79	0.34	0.04	65	0.32	0.08	50
P.W.–3 ×	0.91	0.15	0.77	0.18	82	0.71	0.08	77	0.82	0.20	86	0.75	0.17	76
D.Y.–2 ×	0.78	0.08	0.71	0.18	80	0.64	0.18	73	0.75	0.21	84	0.60	0.17	75
D.Y.–2 ×	0.82	0.13	0.68	0.11	83	0.68	0.21	73	0.71	0.20	85	0.62	0.24	72
P.W.–2 ×	0.95	0.14	0.91	0.13	89	0.88	0.13	77	0.95	0.17	95	0.91	0.25	93
P.W.–2 ×	0.96	0.20	0.96	0.19	95	0.89	0.10	78	0.95	0.17	96	0.81	0.17	78
P.W.–2 ×	0.36	0.10	0.57	0.14	78	0.28	0.05	43	0.47	0.10	67	0.20	0.01	38
E.G.–2 ×	a	a	a	a	90	a	a	58	a	a	88	a	a	46
E.G.–2 ×	a	a	a	a	81	a	a	63	a	a	86	a	a	57
E.G.–2 ×	a	a	a	a	88	a	a	49	a	a	a	a	a	a

Detection and identification data. Each row gives the results of three consecutive sessions for one subject (a triad of sessions). The left column gives hit and false alarm rates for detection when $M = 1$. The other four columns give both hit and false alarm rates for detection, and proportion correct identification, when $M = 2$ or $M = 4$. The data were pooled across spatial frequencies. Only data from the first 9 rows were used in figures 5 and 6. (Cells marked *a* indicate that data were not collected for that condition for that subject.) D.Y.–3 × ran under two different contrasts. Rows 1 and 2 are the results for the higher contrast; rows 3 and 4 the lower contrast. In all other cases one contrast was used for each observer with each group.

results are given in separate columns for the blocks where two frequencies ($M = 2$) were intermixed and the blocks where four frequencies ($M = 4$) were intermixed.

In Table 2 and in the analyses described below (those connected with Figs 3, 4, and 5) results were pooled across spatial frequencies within any one session before computing hit and false alarm rates and proportion correct identification. Since contrasts were set to give approximately equal levels of performance on all four frequencies, such pooling should only reduce the variability of the results, at least if models like those described above are correct. In fact, many of the analyses described below were also done for individual frequencies in individual sessions; the conclusions reached were the same as with the pooled data, and there were no systematic trends across spatial frequency.

Identification performance in different set sizes

Figure 3 shows the proportion of correct identification in the four-frequency intermixed condition ($M = 4$) on the vertical axis and the proportion of correct identification in the two-frequency intermixed condition ($M = 2$) on the horizontal axis. The solid symbols come from cases showing no systematic confusions; the open symbols from the other cases.

The upper straight line on the figures shows where the results would lie if performance were the same in both the two-frequency ($M = 2$) and four-frequency ($M = 4$) intermixed conditions, that is, if there were no uncertainty effects. The bottom curve (marked "boundary") is explained later.

The two curved lines (marked "Gaussian" and "Exponential") are predictions from the independent-channels models described above assuming the equal-variance Gaussian or the exponential distribution. (Detection rule is irrelevant in this comparison since only identification results are involved.) Note that both models predict that performance in the four-frequency condition should be

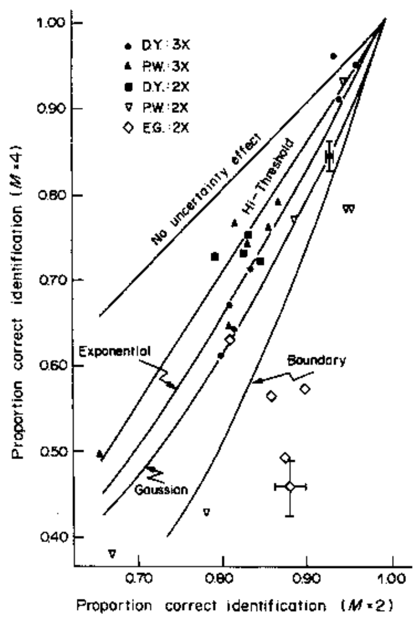

Fig. 3. Proportion of correct identification with four frequencies intermixed ($M = 4$) vs proportion of correct identification with two stimuli intermixed ($M = 2$). Each point is from one session, with data pooled across frequencies, 400 trials per point. The two points with error bars illustrate ±1 SE computed from the binomial distribution. The solid curves are explained in the text. Solid symbols indicate cases where there were no systematic confusions. Open symbols indicate cases where there were systematic confusions.

worse than that in the two-frequency condition. The exponential model may fit the results from the unconfused cases somewhat better than the Gaussian: all the solid points are on or above the Gaussian curve but rather equally distributed around the exponential.

Predictions of a high-threshold independent-channels model are also shown in Fig. 3. Such models are clearly wrong (see Discussion) and will not be pursued further here, but it seemed worth noting that they do predict uncertainty effects in identification although not in detection. (When the stimulus is not detected, the observer's chance of identifying correctly by guessing is higher in smaller set sizes.) The predicted effects are somewhat smaller than those actually obtained in this study, however.

Many probability distributions might be considered in the model described above in addition to Gaussians and exponentials. It is possible to compute a bound on their predictions for the uncertainty effect in identification (Shaw, 1980). The lowest curve in Fig. 3 is the lower boundary of the region in which independent-channels models' predictions can fall no matter what continuous probability distribution is assumed. Therefore, if data points fall significantly below this boundary line, the uncertainty effect is too large to be explained by any independent-channels models like those described above, no matter what probability distribution is assumed.

In Fig. 3, the results from cases where there were no systematic confusions were all above the boundary line. That is, the identification uncertainty effect can be explained by noise-limited models, and there is no need to postulate a limit to attention capacity. The results from cases where there were systematic confusions tended to fall below the boundary line, particularly the results from E.G.-2X where the systematic confusions were greatest (see Fig. 2). This is further evidence that the assumptions of the above independent-channels model have been violated in these cases. The stimuli may be too close to stimulate separate channels (violating assumption 2) and/or there may be confusions among neighboring channel outputs at higher-levels of the nervous system (violating assumption 6). In either kind of violation, points might fall below the boundary line since, in the four-frequency intermixed blocks, a middle frequency has two neighbors, those on either side of it, whereas in the two-frequency intermixed blocks, each frequency has only one neighbor.

If attention capacity is limited so that an observer cannot monitor all channels perfectly (a violation of assumption 4) the results might also fall below the boundary line. This explanation is unattractive here, however, for it seems unlikely that P.W. could monitor four channels perfectly for spatial frequencies a factor of three apart but not for a factor of two. In other situations, however, results below the boundary line seem likely to indicate an inability to monitor all relevant channels perfectly, e.g. the results for identifying the location of a target letter appearing amid distractors (Shaw, 1983).

To summarize, identification performance did deteriorate as set size increased. For cases where there was no systematic confusion in the identification responses, the size of this uncertainty effect was consistent with the independent-channels models (assumptions 1–6). For cases where there were systematic confusions, the identification uncertainty effects were too large to be explained by any independent-channels model (assumptions 1–6 above) probably because the frequencies were too close to stimulate completely separate channels.

Computation of underlying model parameters

The type of comparison shown in Fig. 3 requires plotting performance data directly on each axis. This is not possible in the case of our detection data where two numbers (hits and false alarms) are needed. The comparisons involving detection results are presented in a different form, therefore. For each model and each of the five kinds of performance data, we calculated the value of the underlying parameter that would lead that specific model to predict the obtained performance. This underlying parameter describes the signal and noise distributions in each individual channel. It is $\underline{k}' = 2\ \log_{10}(1/k)$ in the case of exponential-distribution models and $\underline{d}' = (\mu_s - \mu_n)/\sigma_n$ in the case of Gaussian-distribution models. Since all spatial frequencies are presumed equally detectable in these analyses, this parameter is the same for each of the M channels and thus one parameter is sufficient to describe the model.

To assess how well a specific model does in relating any two kinds of performance data, we can plot the underlying parameter from one kind of data against the underlying parameter from the other kind. If the specific model were a perfect description of the system, then the two underlying parameter estimates should be the same (except for statistical variability) and the plotted points should lie close to the positive diagonal. Such comparisons are given in Fig. 4 and are discussed in the next sections.

Since the systematic confusions shown in Fig. 2 and the large uncertainty effects shown in Fig. 3 indicate violations of the models' assumptions, results from the two cases E.G.-2X and P.W.-2X are not presented in Figs 4 or 5 below. (Those from E.G.-2X could not be in any case since detection results were not collected from him.) As it happens, when plotted in the form of Figs 4 or 5, they do not deviate systematically from the points for the cases shown.

Detection performance in different set sizes

In the middle row of panels of Fig. 4 we compare detection performance when $M = 4$ (underlying parameters plotted on the vertical axis) to that when $M = 2$ (underlying parameters plotted on the horizontal axis). The points in the left middle panel tend to lie above the positive diagonal. That is, the adding-of-Gaussians model predicts systematically larger detection uncertainty effects than were found. (Points above the positive diagonal reflect an underlying parameter for the $M = 2$ condition that is smaller than that for the $M = 4$ condition. Thus the adding-of-Gaussians model that correctly predicts the observed performance in the $M = 2$ condition would predict worse performance than observed in the $M = 4$ condition.) The points for the maximum-Gaussian and maximum-exponential models (middle and right panels), on the other hand, lie quite close to the diagonal indicating that these models predict effects of about the right size.

The bottom row of panels compares detection performance when $M = 2$ to that when $M = 1$. Here the points in the rightmost panel, for the maximum-exponential model, tend to lie below the diagonal. That is, the maximum-exponential model predicts smaller detection uncertainty effects than were found going from $M = 1$ to $M = 2$. The maximum-Gaussian and adding-of-Gaussian models, on the other hand, predict effects of about the right size.

Not shown are the graphs comparing detection performance in $M = 1$ to $M = 4$. They are implicit in the graphs shown for $M = 1$ to $M = 2$ (bottom row) and $M = 2$ to $M = 4$ (middle row), and produce what one might expect. The adding-of-Gaussians predicts too large an effect (since it does so from $M = 2$ to $M = 4$), the maximum-exponential too small an effect (since it does so from $M = 1$ *to* $M = 2$) and the maximum-Gaussian approximately the observed effect.

To summarize, in cases where there are not systematic confusions in Fig. 2, the size of the detection uncertainty effects in going from $M = 1$ to $M = 2$ to $M = 4$ is generally consistent with the class of independent-channels models. Of the three specific versions we have considered, the maximum-Gaussian best accounts for uncertainty effects in detection.

Identification and detection performances in the intermixed conditions

The top row of Fig. 4 compares identification performance when $M = 4$ (underlying parameters plotted on the vertical axis) to detection performance

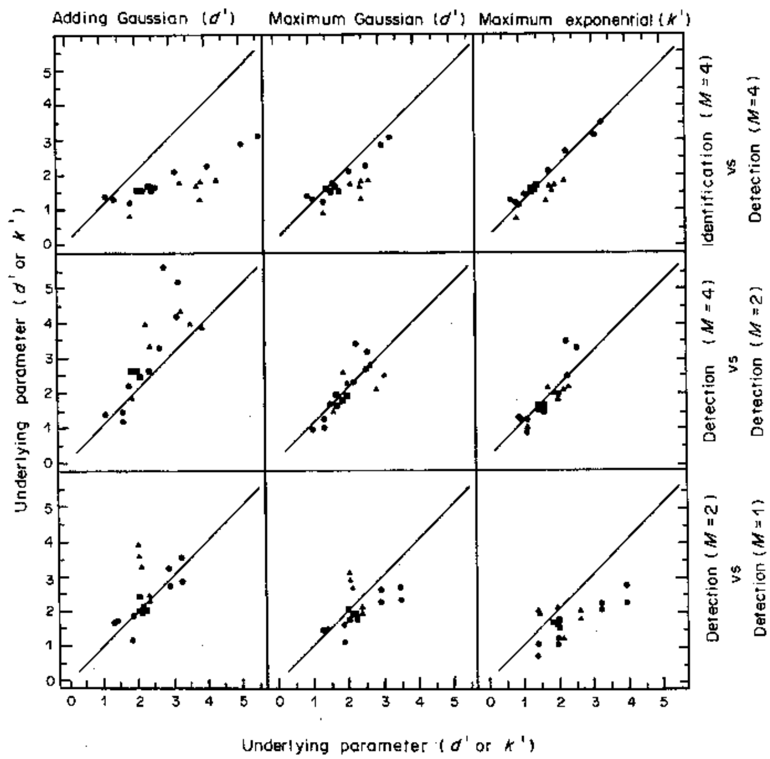

Fig. 4. For 3 models (columns) the values of $\underline{d}'$ or $\underline{k}'$ for three different comparisons (rows) are calculated from the data. The horizontal axis plots Detection, $M = 4$ (top row); Detection, $M = 2$ (middle row); or Detection, $M = 1$ (bottom row). The vertical axis plots Identification, $M = 4$ (top row); Detection, $M = 4$ (middle row); or Detection, $M = 2$ (bottom row). Data points are from single sessions, pooled across frequencies, 400 trials per point.

in the same sessions, that is, when $M = 4$ (horizontal axis). Both the adding-of-Gaussians (left panel) and maximum-Gaussian model (middle panel) predict that identification of stimuli at a given level of detection performance should be better than it is. The points for the maximum-exponential model (right panel), however, lie quite close to the positive diagonal, indicating that this model accounts well for the observed relation between identification and detection performance in intermixed sessions.* Although not shown, analogous plots for identification vs detection performance when $M = 2$ look extremely similar.

Summary of comparison with models

As a class, the independent-channels models described above do a good but certainly imperfect job of accounting for the detection and identification performances in cases where there were not systematic confusions.

Perhaps the easiest way to remember the details of the preceding comparisons with models is to note that the maximum-exponential model (which, of the models considered here, predicts the smallest uncertainty effects) correctly accounts for all the relationships among detection and identification performances in the intermixed conditions (Fig. 3 and the top and middle rows of Fig. 4). Remember, however, that it predicts too small an uncertainty effect in going from $M = 1$ to $M = 2$ (bottom row Fig. 4). In other words, it predicts that detection performance in the alone condition ($M = 1$) should be worse than it is relative to the other four kinds of performance data.

Detection performance in the alone condition ($M = 1$) can be successfully related to detection performance in the intermixed conditions ($M = 2$ and 4) by the maximum-Gaussian. But this model fails at relating detection to identification in the intermixed conditions.

*A number of investigators interested in the relation of detection to identification performance in various stimulus domains (e.g. Green *et al.*, 1977; Swensson and Judy 1981; Parasuraman and Beatty, 1980; Swets *et al.*, 1978) have made use of the theorem of Starr *et al.* (1975) in the way described by Green and Birdsall (1978) This theorem is attractive because it allows one to test a large class of independent-channels models against detection and identification results collected in the same intermixed session. This class of models assumes a maximum-output identification rule (with the same criterion in each channel). No assumption about the form of the probability distribution is necessary except that it is continuous. This distribution is, in effect, deduced from the ROC curve. (The stimuli must be equally detectable and far enough apart to affect separate channels. The channels are probabilistically independent; the observer monitors perfectly.) If we had collected full ROC curves they would presumably have been rather well described by the maximum-exponential model. Since the maximum-exponential model is successful at relating identification to detection performance in intermixed blocks, the Starr *et al.* theorem would presumably have been successful also.

Thus, as discussed further in the next section, there is one (and only one) failure that is common to all versions of the independent-channels models we have considered: no model we have considered can successfully relate detection performance in the alone blocks ($M = 1$) to identification performance in the intermixed blocks ($m = 2$ *or* 4).

Detection performance in the alone condition ($M = 1$) and identification performance

This failure of the models is shown directly in Fig. 5. The underlying parameters describing detection when $M = 1$ are plotted on the horizontal axis with the Gaussian case in the left panel and the exponential case in the right panel. Proportion of correct identification when $M = 4$ is plotted on the vertical axis. The predictions of the models are given by solid lines. In both panels, the obtained identification performances fall below the predicted performances by about 0.1. The failures in the case of $M = 2$ are very similar to those shown.

This failure should not be overemphasized, however. The discrepancy between model predictions and experimental results (about 0.1 on the vertical proportion correct axis, about 0.5 on the horizontal underlying parameter axis) is small relative to the ranges over which proportion correct and d' or k' vary. As is clear in Fig. 5, identification performance is increasing across the same range of contrasts for which detection performance increases.

DISCUSSION

Systematic confusions

As was expected on the basis of independent-channels models for far-apart stimuli, there were no systematic confusions among the identification responses to spatial frequencies a factor of three apart or, for one observer, a factor of two apart. There were systematic confusions among the responses to spatial frequencies a factor of two apart for two observers.

Detection and identification

For far-apart spatial frequencies, the class of independent-channels models explains quite well the quantitative details of the detection and identification of gratings of far-apart spatial frequencies (Figs 2–5). Of the three models explicitly compared to the results, the maximum-exponential model did perhaps the best job, successfully accounting for the relationships among detection and identification performances in both the intermixed conditions. With the exponential distribution, it makes little difference whether the maximum-output or adding-of-outputs detection rule is used, and an Adding-of-Exponentials model would do just as well. The Maximum-Gaussian model also did a good job, accounting rather well for detection performances in all three set sizes although failing to exactly relate

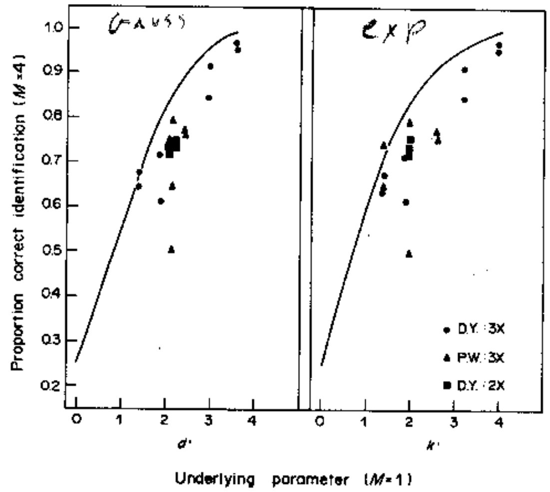

Fig. 5. Proportion of correct identification with four frequencies intermixed ($M = 4$) vs $\underline{d}'$ or $\underline{k}'$ with one frequency ($M = 1$). Left panel: Gaussian distributions. Right panel: exponential distributions. Data points are from single sessions, pooled across frequencies, 400 trials per point.

identification to detection. The adding-of-Gaussians model did not do as well as the other two, basically because it predicts larger uncertainty effects than occur when increasing the set size from 2 to 4.

Attention

In short, even in the potentially more difficult task of identification of spatial frequencies, there is no need to assume a limited attention capacity, just as there had not been in detection.

Note that, although attention capacity may be unlimited, the observer may still selectively attend to one or a small group of channels when it is to his advantage. In fact, according to independent-channels models, an observer is assumed to monitor only one channel (or one small group of channels) whenever he is certain about the spatial frequency. The spatial-frequency tuning of the detection uncertainty effect in blocks containing a preponderance of one spatial frequency is also evidence that an observer is able to monitor only one or a small group of channels (Davis and Graham, 1981; Davis, 1982). Further, the existence of sequential dependencies in some conditions suggests that switching of attention among channels may occur rather than simultaneous monitoring of all channels if conditions favor it (Davis and Graham, 1981). This switching of attention can apparently take place in less than a second judging from the complete effectiveness of auditory pre-cues (Davis *et al.*, 1983).

Complications in comparing alone to intermixed conditions

A common minor failure of all the independent-channels models is in relating detection in the alone condition ($M = 1$) to identification in the intermixed conditions ($M = 2$ or 4). The maximum-exponential version, in particular, predicts all the other results (all the relations among detection and identification in the intermixed conditions) quite well; detection in the alone condition, however, is too good relative to the other results to be accounted for by that model. The suspicion arises, therefore, of some systematic difference between our alone and intermixed experimental conditions that is violating assumptions of the models, although the assumptions are not wrong in an important way. In this section we consider three possibilities for this difference. Major modifications of the models are considered in the next section.

In the alone condition, the observer made only one response on each trial although making two (both a detection and identification response) in the intermixed conditions. Perhaps this difference allowed the observer to perform generally better in the alone condition than in the intermixed conditions. This possibility cannot be completely ruled out. However, the results in Davis *et al.* (1983), where the observer always made only one response (a detection response) on each trial, show a drop in detection performance between $M = 1$ and $M = 3$ that is large enough to be consistent with the same models that can account for the drop measured here between $M = 1$ and $M = 2$.

In the present experiment, various practical considerations led to the results for the alone condition being gathered in different sessions from those for the intermixed conditions, and generally, therefore, on different days. Since there are slow shifts in sensitivity across days (between-session variability is greater than within-session variability), it is possible that the observers just happened to be consistently more sensitive on their alone days than on their intermixed days, producing artificially large decrements in performance between the alone ($M = 1$) condition and the others. Although possible, it would be rather a coincidence. In any case, the alone and intermixed conditions in Davis *et al.* (1983) were run on the same day.

As mentioned earlier, the assumption that channels are treated identically (implicit in the maximum-output detection and identification rules) is not quite true. At least on some days for some observers, there seem to be different criteria in different channels in the intermixed conditions. Perhaps differential criteria lower performance in the intermixed conditions. (In the alone condition, of course, there is no possibility for differential criteria.) Unfortunately, computing the exact predictions of the models using differential criteria would be a very difficult task. Instead, we did a rough check on the possibility that differential criteria in the intermixed conditions might be causing the failure of the models. We computed two *ad-hoc* measures for each session: one measuring how non-uniform the identification responses to the blank were in that session and the second measuring the discrepancy between predicted and actual identification performances (see Fig. 5). We then correlated these two measures across all sessions. The correlation was trivial and nonsignificant. This analysis, although far from compelling, suggests that differential criteria are not the reason for the minor failure of the models in relating alone detection to intermixed identification.

Other versions of independent-channels models

The models quantitatively studied here are only a sample of the possible independent-channels models. Thus the question naturally arises as to whether other verions of independent-channels models would be as good or even better at explaining the detection and identification of gratings of far-apart spatial frequency.

Other probability distributions. Unequal-variance Gaussian distributions, where the inequality increases with detectability in the way suggested by the slope of empirical ROC curves (see appendix), were studied by Graham *et al.* (1983). With the adding-of-outputs rule, where predictions are not completely determined by the ROC curve for $M = 1$, these unequal-variance Gaussians predict more uncertainty effect in detection than does the exponential and more than was found here. With the maximum-output rule, however, they act very much like the exponential distributions, as would be expected since the ROC curves (for $M = 1$) for the two distributions are known to be very similar. Thus, the unequal-variance Gaussian model with a maximum-output rule would also be a good description of the experimental results reported here.

The double-exponential distribution and the maximum-output detection rule produces a model that is equivalent to the choice model (see Yellott, 1977). It predicts uncertainty effects in both detection and identification that are larger than those predicted by the Maximum-Gaussian model (e.g. Green and Weber, 1980) and inconsistent with the results here. In any case, the double-exponential distribution leads to ROC curves for the alone condition ($M = 1$) that have a slope greater than 1.0 and thus too steep to be compatible with known results (Graham *et al.*, 1983).

Some sample ROC curves for a model assuming Poisson distributions are shown by Nachmias (1972) as well as a plot of their horizontal intercept vs signal strength for several values of M (1, 4, and 16). The predicted size of the detection uncertainty effect (from $M = 1$ to 16) seems similar to that of the maximum-exponential or Gaussian distributions, in fact. Its ROC curves when $M = 1$, however, are close to slope one (like the equal-variance Gaussian) which makes them somewhat less attractive as a description of visual pattern thresholds.

High-threshold independent-channels models are like the models described above but with a two-discrete-state probability distribution and no false alarms. They predict no uncertainty effects in detection, and thus must be wrong in detail at least. They also predict ROC curves that are inconsistent with available data. It is somewhat odd, therefore, that the Quick Pooling model, which as usually derived is a high-threshold model, does so well at relating the detection thresholds of different visual patterns (see further discussion of this issue in Davis *et al.*, 1983).

In low-threshold models there are only a small number of discrete states that channel responses can take on but, unlike high-threshold models, there is some probability that noise will cause a channel to be in the highest detect state. These models do predict uncertainty effects depending on the parameters chosen for the probabilities of getting into each state (Green and Weber, 1980; Green and Birdsall, 1978). For a given level of detectability, they can predict identification performance as high as that predicted by continuous models or a good deal lower depending on the exact parameters and detection rule (Green and Birdsall, 1978). These models predict ROC curves that have unnatural looking corners in them, but one might well never see those corners in empirical results. Certain one-parameter families of these two-state distributions can be ruled out as an explanation of our results. The symmetric two-state model of Green and Weber, 1980, for example, predicts detection uncertainty effects on the negative diagonal that are too large for the present results. It would be a mistake to think that all two-state models could be ruled out at this stage as an explanation of uncertainty results, however, and certainty multiple-state models could not be.

Modifications of other assumptions

Allowing for differential criteria in different channels and also for variability in that criterion across time would be more realistic. As suggested by the identification of individual frequencies in compound gratings (Hirsch *et al.*, 1982; Olzak, 1982) the responses of different channels might be positively correlated to some extent, at least at low signal levels. Positive correlation among the responses would reduce the size of predicted uncertainty effects predicted by any model, whereas negative correlation would increase it. These studies further suggested that there might be some inhibition among channels, another factor that would decrease predicted uncertainty effects. Or, as in an alternate explanation of compound-grating identification results, the correct linking hypotheses might be more complicated than the ones assumed here. Finally, the number of channels presumed to be monitored in the different set sizes might be wrong. In a set size of one, for example, the observer might manage to monitor only the relevant channel. But when the set includes two or four far-apart frequencies, the observer monitors some irrelevant channels as well.

It is probable that some combination of the modified versions of assumptions 1–6 would produce an independent-channels model that could account for the experimental results even better than the versions considered here. We have been unable to think of a simple or elegant modification of the models that would do so, however, and the discrepancies between these models and the experimental results seem too small to justify complicated modifications. On the other hand, numerous combinations of minor modifications would undoubtedly produce independent-channels models that do just as well or better than as the versions considered here.

Acknowledgements—Part of this work was presented at the meeting of the Association for Research in Vision and Ophthalmology, 1981. This research was partially supported by a grant from the Foundation of the Optometric Center of New York, and NSF Grant number BNS-83-11350 to Dean Yager, and NSF Grant number BNS-76-18839 to Norma Graham. The authors wish to thank Jeanette Churche for her work as a research assistant. We regret to say that Marilyn Shaw died on 13 November 1983.

REFERENCES

Bergen J. R., Wilson H. R. and Cowan J. O. (1979) Further evidence for four mechanisms, mediating vision at threshold: Sensitivities to complex gratings and aperiodic stimuli. *J. opt. Soc. Am.* **69**, 1580–1586.

Bush R., Galanter E. and Luce R. D. (1963) Characterization and classification of choice experiments. In *Handbook of Mathematical Psychology* (Edited by Luce, Bush and Galanter). Wiley, New York.

Campbell F. W. and Green D. B. (1965) Optical and retinal factors affecting visual resolution. *J. Physiol.* **18**, 576–593.

Creelman C. D. (1960) Detection of signals of uncertain frequency. *J. acoust. Soc. Am.* **32**, 805–810.

Davis E. T. (1981) Allocation of attention: Uncertainty effects when monitoring one or two visual gratings of noncontiguous spatial frequencies. *Percept. Psychophys.* **29**, 618–622.

Davis E. T. and Graham N. (1981) Spatial frequency uncertainty effects in the detection of sinusoidal gratings. *Vision Res.* **21**, 705–712.

Davis E. T., Kramer P. and Graham N. (1983) Uncertainty about spatial frequency, spatial position, or contrast of visual patterns. *Percept. Psychophys.* **33**, 20–28.

Egan J. (1975) *Signal Detection Theory and ROC Analysis.* Academic Press, New York.

Furchner C., Thomas J. and Campbell F. W. (1977) Detection and discrimination of simple and complex patterns at low spatial frequencies. *Vision Res.* **17**, 827–836.

Graham N. (1977) Visual detection of aperiodic spatial stimuli by probability summation among narrow band channels. *Vision Res.* **17**, 637–652.

Graham N., Kramer P. and Yager D. (1983) Explaining uncertainty effects and probability summation. In *Invest. Ophthal. visual Sci., Suppl.* **24**, 186.

Graham N., Robson J. G. and Nachmias J. (1978) Grating summation in fovea and periphery. *Vision Res.* **18**, 815–826.

Green D. M. and Birdsall T. G. (1978) Detection and recognition. *Psychol. Rev.* **85**, 192–206.

Green D. M. and Swets J. A. (1974) *Signal Detection Theory and Psychophysics.* Wiley, New York.

Green D. M. and Weber D. L. (1980) Detection of temporally uncertain signals. *J. acoust. Soc. Am.* **67**, 1304–1311.

Green D. M., Weber D. L. and Duncan J. E. (1977) Detection and recognition of pure tones in noise. *J. acoust. Soc. Am.* **62**, 948–954.

Hacker M. J. and Ratcliff R. (1979) A revised table of *d'* for M-alternative forced choice. *Percept. Psychophys.* **26**, 168–170.

Hirsch J., Hylton R. and Graham N. (1982) Simultaneous recognition of two spatial-frequency components. *Vision. Res.* **22**, 365–375.

Luce R. D. (1963) Detection and recognition. In *Handbook of Mathematical Psychology* (Edited by Luce R. D., Bush R. R. and Galanter E.), Vol. I, pp. 103–189. Wiley, New York.

Mostafavi H. and Sakrison D. J. (1976) Structure and properties of a single channel in the human visual system. *Vision Res.* **16**, 957–968.

Nachmias J. (1972) Signal detection theory and its application to problems in vision. In *Handbook of Sensory Physiology* (Edited by Jameson and Hurvich), Vol. VII/40. Springer, Berlin.

Nachmias J. (1974) A new approach to bandwidth estimation of spatial frequency channels. In *Invest. Ophthal. visual Sci., Suppl.*

Nachmias J. (1981) On the psychometric function for contrast detection. *Vision Res.* **21**, 215–233.

Nachmias J. and Kocher E. (1970) Visual detection and discrimination of luminance increments. *J. opt. Soc. Am.* **60**, 382–389.

Nachmias J. and Weber A. (1975) Discrimination of simple and complex gratings. *Vision Res.* **15**, 217–224.

Nolte L. W. and Jaarsma D. (1967) More on the detection of one of M orthogonal signals. *J. acoust. Soc. Am.* **41**, 497–505.

Olzak L. A. (1981) Interactive properties of spatially tuned analyzers. In *Invest. Ophthal. visual Sci., Suppl.* **21**, 124.

Olzak L. A. (1982) Inhibition: Effects on grating detection and identification. In *Invest. Ophthal. visual Sci., Suppl.* **22**, 206.

Parasuraman R. and Beatty J. (1980) Brain events underlying detection and recognition of weak sensory signals. *Science* **210** 80–83.

Quick R. F., Mullins W. W. and Reichert T. A. (1978) Spatial summation effects on two-component grating thresholds. *J. opt. Soc. Am.* **68**, 1, 116–121.

Shaw M. L. (1980) Identifying attentional and decision-making components in information processing. In *Attention and Performance VIII* (Edited by Nickerson). Erlbaum Hillsdale, NJ.

Shaw M. L. (1982) Attending to multiple sources of information: I. The integration of information in decision making. *Cogn. Psychol.* **14,** 353–409.

Shaw M. L. (1983) Division of attention among spatial locations: a fundamental difference between detection of letters and detection of luminance increments. In *Attention and Performance X* (Edited by Bouma and Bonwhuis) Erlbaum, Hillsdale, NJ.

Smith J. E. K. (1982) Simple algorithms for M-alternative forced-choice calculations. *Percept. Psychophys.* **31,** 95–96.

Starr S. J., Metz C. E., Lusted L. B. and Goodenough D. J. (1975) Visual detection and localization of radiographic images. *Radiology* **116,** 533–538.

Swensson R. G. and Judy P. F. (1981) Detection of noisy visual targets: Models for the effects of spatial uncertainty and signal-to-noise ratio. *Percept. Psychophys.* **29,** 521–534.

Swets J. A. (1964) *Signal Detection and Recognition by Human Observers.* Wiley, New York.

Swets J. A., Green D. M., Getty D. J. and Swets J. B. (1978) Signal detection and identification. *Percept. Psychophys.* **23,** 275–284.

Thomas J. P. and Barker R. A. (1977) Bandwidths of visual channels estimated from detection and discrimination data. *J. opt. Soc. Am.* **10,** 1408.

Thomas J. P., Gille J. and Barker R. A. (1982) Simultaneous visual detection and identification: Theory and data. *J. opt. Soc. Am.* **72,** 1642–1651.

Watson A. B. (1982) Summation of grating patches indicates many types of detector at one retinal location. *Vision Res.* **22,** 17–26.

Watson A. B. and Robson J. G. (1981) Discrimination at threshold: Labelled detectors in human vision. *Vision Res.* **21,** 1115–1122.

Yellott J. (1977) The relationship between Luce's choice axiom, Thurstone's theory of comparative judgment, and the double-exponential model. *J. math. Psychol.* **15,** 109–144.

APPENDIX

Calculating predictions from models

All the models discussed here obey assumptions (1)–(6) above with the distinctions lying in the particular form of probability density used in assumption (2) and the detection rule in assumption (5).

Let $f(z/\text{noise})$ be the probability density function for the response of a single channel when noise is presented. Let $f(z/\text{signal})$ be the probability density function for the response of a single channel when a stimulus exciting that channel is presented. [Since the contrasts of the four frequencies used in these experiments were chosen to make the frequencies equally detectable, the same signal probability density function $f(z/\text{signal})$ applies to all four channels involved in any prediction.] Then let x and y (which will be the predicted false-alarm and hit rate when the set size is one) be the integrals of these two density functions from some criterion lambda to infinity. That is

$$x = \int_{\lambda}^{\infty} f(z/\text{noise})\,dz$$

and

$$y = \int_{\lambda}^{\infty} f(z/\text{signal})\,dz.$$

When the density functions are Gaussians, x and y must be found from a table (or directly from numerical integration). When the density function is an exponential $\exp(-kx)$, however, integration can be done analytically and easily and yields

$$x = \exp(-\lambda)$$
$$y = \exp(-k\lambda).$$

Predictions for detection performance

Alone condition ($M = 1$). In the alone condition, x and y equal the predicted false-alarm and hit probabilities (that is, the predicted probabilities of saying yes when noise or signal is presented, respectively) for a particular criterion lambda. The full ROC curve is generated by varying lambda. This is true for either the adding-of-outputs or maximum-output detection rule since they reduce to the same rule for the alone conditon.

As is well-known and easy to derive, the ROC curve for the case of Gaussian density functions is a straight line on probability coordinates (that is, when the z-scores of x and y are plotted). Its slope is equal to the noise standard deviation divided by the signal standard deviation (σ_n/σ_s).

The absolute value of its horizontal intercept is equal to the value of the parameter $\underline{d}'$, that is, the difference between the means of the signal and noise density functions divided by the standard deviation of the noise distribution $[(\mu_s - \mu_n)/\sigma_n]$. At the intersection of the ROC curves with the negative diagonal, twice the ordinate (what we will call the negative diagonal d') is equal to the difference between the means divided by the average of the two standard deviations $[(\mu_s - \mu_n)/s]$ where $s = [(\sigma_s + \sigma_n)/2]$. Notice that the negative-diagonal d' equals $\underline{d}'$ only for the case of equal signal and noise standard deviations (where the ROC curve has a slope of one).

The ROC curve when $M = 1$ for the exponential case is easy to derive (Green and Swets, 1974; Egan, 1975) and is $y = x^k$. This function turns out to be almost linear when plotted on probability coordinates for false-alarm probabilities within an empirically-collectable range. Further, the value of twice the ordinate at the intercept with the negative diagonal (what is called negative-diagonal $\underline{d}'$ for the Gaussian model) is approximately equal to $\underline{k}' = 2\log_{10}(1/k)$. In fact, to get exponential-model ROC curves with apparent negative-diagonal d' values (twice the ordinate at the negative-diagonal intersection) equal to 3.00, 2.00, and 1.00, one needs k' values equal to 3.18, 2.15, and 1.01, respectively.

The ROC curves for the exponential distribution get shallower as the detectability of the stimulus increases. To describe this trend and compare it with that in empirical results, consider a plot of the reciprocal of the exponential ROC curve's slope in the upper left quadrant (on z-axes) as a function of the horizontal intercept. (If ROC curves came from Gaussians of unequal variance, this plot would be a plot of (σ_s/σ_n) vs $\underline{d}' = [(\mu_s - \mu_n)/\sigma_n]$. For the exponential curves, one finds the following relation: the reciprocal of the slope is approximately equal to one plus a constant times the horizontal intercept. That constant is about one-third when describing the relationship for horizontal intercepts out to about -3.0 (which occur with a k' value of about 2.0) but smaller (about one-fourth) when describing the relationship over a larger range (out to intercepts of about -5.0).

Empirical ROC curves for many stimuli also seem to get shallower with increased detectability (Green and Swets, 1974; unpublished results for sinusoidal gratings from a study reported in Hirsch *et al.*, 1982; Nachmias and Kocher, 1970). In fact, their trend is frequently described by saying that the reciprocal of the slope is approximately equal to one plus one-fourth times the horizontal intercept. Given the imprecision in the empirical results, constants of 1/3 or 1/5 would do as well as 1/4. Thus, the exponential ROC curves seem to agree quite well with empirical results for simple stimuli.

Intermixed conditions. Maximum-output detection rule. Let x_M and y_M be the false-alarm and hit rates, respectively, in the condition where M frequencies are intermixed. Then, if an observer says yes whenever the maximum output (or, equivalently, the output in at least one channel) is greater than the criterion lambda

$$x_M = 1 - (1 - x)^M$$

and

$$y_M = 1 - (1 - y)\,(1 - x)^{M-1}.$$

Full ROC curves can be generated for any given value of M and for any given probability density functions by varying lambda. (Note that lambda is being assumed equal for all channels in accord with the maximum-output rule.) For $M = 2$ and for $M = 4$, we generated curves for a range of values of $\underline{k}'$, assuming exponential density functions, and of $\underline{d}'$, assuming equal-variance Gaussians. For the Gaussians, these curves are published in Nolte and Jaarsma (1976).

Intermixed condition. Adding-of-outputs detection rule. The adding-of-outputs detection rule is particularly easy to use in combination with Gaussian density functions (e.g. Creelman, 1960). For, as is well-known, the sum of Gaussian-distributed random variables is again Gaussian distributed. The mean is the sum of the means, and, if the random variables are probabilistically independent, as the channel outputs are assumed to be, the variance is the sum of the variances. Thus the ROC curves are linear on z-axes with easily computable intercepts and slopes. In particular, setting the mean and standard deviation of the noise distribution equal to 0 and 1, respectively, (without loss of generality) and letting $d'_e(M)$ be the negative-diagonal $\underline{d}'$ value for M intermixed frequencies

$$d'_e(M) = \frac{2\,\mu_s}{(\sigma_s^2 + M - 1)^{0.5} + (M)^{0.5}}.$$

It is easy to show that $d'_e(M)$ is greater than or equal to $d'_e(1)/\sqrt{M}$. equality holding when $\sigma_s = \sigma_n = 1$.

In general, the density function for the sum of random variables is the convolution of the individual density functions for those random variables. In the case of exponential distributions, these convolutions can be calculated in a fairly straightforward manner. For a noise trial in a condition of M intermixed frequencies, the convolution of M exponentials with $k = 1$ is needed. For a signal trial, the convolution of $M - 1$ exponentials with $k = 1$ and one exponential with k less than 1 is needed. The densities can then be analytically integrated from lambda to infinity to yield the false-alarm and hit rates.

Predictions for identification performance

For continuous probability distributions like those discussed here, the relation between proportion correct in the identification of M intermixed frequencies and the ROC curve for detection in the alone condition ($M = 1$) is well-known (e.g. Green and Birdsall, 1978; Green and Swets, 1974; pp. 45–51). Letting $P(M)$ equal the proportion of correct identification in the condition where trials of M frequencies are intermixed, the independent channel models predict

$$P(M) = \int_0^1 (1 - x)^{M-1}\,dy.$$

This is often known as the area theorem since, when $M = 2$ this integral is equivalent to the integral of y with respect to x, that is, the area underneath the ROC curve.

For the Gaussian density functions, the values of these integrals must be obtained numerically. They have been tabled for the equal-variance case (Elliot's table, in Green and Swets, 1974, recently improved by Hacker and Ratcliff, 1979), and an algorithm for extending them has been suggested by Smith (1982).

For the exponential density function, the integration can be done analytically and yields

$$P(2) = 1/(k + 1)$$
$$P(4) = 1 - 3k/(k + 1) + 3k/(k + 2) - k/(k + 3)$$